(There was no Reviewer 1)

Reviewer 2

In "Volatile organic compound fluxes in the San Joaquin Valley – spatial distribution, source attribution, and inventory comparison", authors Pfannerstill et al. report on the results of airborne (emission) flux measurements of VOCs in the San Joaquin Valley in California. The results are compared to emissions inventories and attributed to source types, revealing important mismatches, in particular underestimated or missing point sources.

Overall, the manuscript is well structured and clearly written. It is to the point and very pleasant to read. The methodology is sophisticated and makes excellent use of a (probably) unique observational dataset that appears carefully acquired. The results are generally solid, and discussions and conclusions well supported. A particular highlight is the authors' careful work in attributing airborne flux measurements to respective emission sources via flux footprint disaggregation. Also, various exiting inventories were considered and specific additions to inventories proposed.

All in all, that makes for interesting results, which will be very useful -- for emissions modeling and air quality studies (especially for the San Joaquin Valley), as well as flux measurement endeavors. In conclusion, I warmly recommend this study for publication in Atmospheric Chemistry & Physics.

I do have a few comments/questions, which mostly relate to occasional wishes for a bit more details or clarifications. Almost all of them concern the methods descriptions and analysis approaches. I list them below, starting with 4 somewhat bigger comments, followed by a list of minor and technical comments. However, I expect that addressing these will only require minor revisions or clarifications.

We thank the referee for their positive assessment and thoughtful comments which have helped to improve the manuscript. Responses below in blue, changes to the manuscript in red.

Main comments:

(1)

L202-203: "A running mean of 2 km was applied to the 10-Hz fluxes to eliminate turbulence effects causing artificial emission and deposition, and sub-sampled to 200 m."

I am not completely following here. What did the sub-sampling procedure consist of? What is the nature of the artifacts that were sought to be avoided? (Vertical aircraft motion?) And how did those artifacts manifest and how was it judged (or decided) that a 2-km running averaging (plus possibly that subsampling) would successfully deal with them?

It could be worth to also illustrate that process in a supplement figure.

We agree that this point would benefit from some clarification. Applying a running or moving average is common in airborne flux studies, and has been reported by e.g. (Wolfe et al., 2015; Schobesberger et al., 2023; Wolfe et al., 2018). When the aircraft flies through an eddy, it may only sample its upward or only its downward movement. Only by averaging is it possible to obtain the net surface fluxes. The running mean procedure is thus applied to eliminate the effects of small-scale turbulence that causes artificial up-and downward fluxes at the sampling timescale. Wolfe et al. (2015) describe the reasoning as "to remove some of the variability associated with sampling individual strong eddies and better represent surface conditions". The 2 km were chosen for averaging because this is the scale of the eddy size as observed in the cospectrum (see Fig. S1b). After the application of the running mean, subsampling was performed because the running mean keeps the original time resolution, but this made the dataset too large to handle. 200 m resolution was deemed reasonable to be able to match emissions to sources. A graphical depiction of this process is shown in (Zhu et al., 2023), Fig. 1c (pasted below).

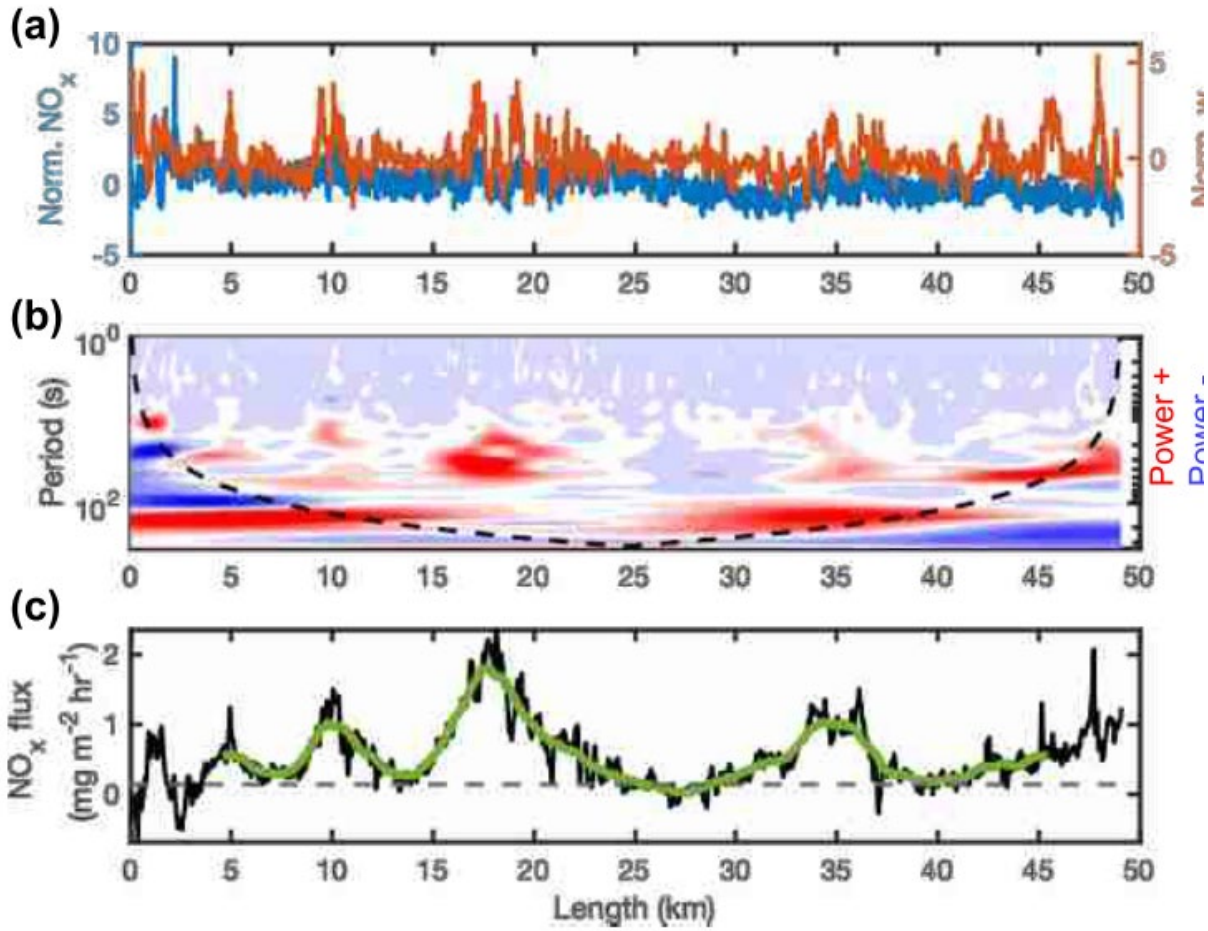

Figure R1. a) The variance of NOx and vertical wind speed, b) frequency and time-resolved wavelet power spectrum with the cone of influence shown as a black dotted line, c) the integrated fluxes from the raw data points are shown in black, the fluxes after moving averaging and COI filtering are shown in green. The dashed gray line indicates the detection limit of this segment.

We adapted the text as follows:

"Averaging is necessary to obtain net fluxes, since the movement of the aircraft through small eddies can cause artifacts by sampling only the upward- or only the downward flux of an eddy at the sampling timescale. Therefore, it is common to integrate airborne fluxes at the scale of peak turbulence (e.g. (Wolfe et al., 2018; Schobesberger et al., 2023). A running mean of 2 km (the peak scale of the sampled eddies (Fig. S1b)) was applied to the 10-Hz fluxes to eliminate the effects of small-scale eddies that would otherwise cause artificial emission and deposition. Since the moving average preserves the original time resolution which is not meaningful for the analysis and difficult to handle, we then sub-sampled the data to 200 m."

(2)

2.5.6

From reading Wolfe et al. (2018; in particular Section 3.4.2 therein), I have come to the understanding that the methods referenced and used here for estimating/calculating flux errors (in particular the random errors) have been developed for "traditional" eddy covariance calculations using ensemble averages, and may not be directly applicable to all CWT fluxes. Also, it does not become clear if the various uncertainties were determined for legs as a whole, or individual CWT fluxes, or some combination thereof.

Could the authors clarify that and comment on the applicability of the methods to their procedure given concerns/proposed methods by Wolfe et al.?

Thanks for making us realize that our description of how and why we calculated uncertainties was not entirely clear. First of all, we did not use the Langford et al. method to calculate flux errors, which would, as the reviewer rightly pointed out, not be applicable to airborne CWT fluxes. We only followed the Langford method to estimate instrument noise, and treated the noise like any other VOC signal to calculate noise-derived CWT fluxes (i.e., flux noise). Errors due to low frequency losses and noise in turbulence sampling were calculated following Lenschow et al. (2014), which are the same equations listed by Wolfe et al. (2018). As Wolfe et al. (2018) pointed out, the Lenschow et al. random flux errors do not include the impact of instrument noise, which is why we propagated the random errors together with the flux noise (derived from the white noise time series), thus addressing the criticism voiced in Wolfe et al. (2018). We hope the following adaptations in the text clarify this:

“The method used for uncertainty calculation is described at length in Zhu et al. (2023). The instrument noise contribution to the flux detection limit was calculated by adapting procedures from Langford et al. (2015). For each VOC and for each flight segment, a VOC white noise time series was created, and wavelet fluxes using this white noise time series and the measured wind were calculated (eq. 10 in Wolfe et al. (2018)). If the resulting random flux was smaller than the random covariance (i.e., covariance at ±220-240 s lag time), the random covariance of the respective segment was used instead of the white noise-derived flux. Thus, a flux detection limit was derived for each segment. The overall precision (random error) was propagated from the 2σ detection limit and the random noise in turbulence sampling which was calculated following Lenschow et al. (1994) (eq. 11 in Wolfe et al. (2018)). The accuracy (systematic error) was propagated from the uncertainty of the calibration, the systematic uncertainty of the flux calculation due to low-frequency losses (eq. 7 in Wolfe et al. (2018), (Lenschow et al., 1994)), and the uncertainties of the divergence corrections. The uncertainty of the chemical vertical divergence correction was estimated to be 20 % of the correction applied. The aggregation of data from multiple time periods caused uncertainty in the determination of the physical vertical divergence slopes. The uncertainty of the physical vertical divergence correction was estimated using a Monte Carlo uncertainty propagation, assuming a 17 % uncertainty each for the slopes and boundary layer heights, since 17 % was the average day-by-day variability in the vertical divergence slopes of benzene. The resulting median uncertainty of the vertical divergence correction was 17 % (average: 51 %). The final uncertainties were unique to each VOC and segment. Precision ranged from 4 %-220 % (for gas standard calibrated VOCs 4-150 %), accuracy from 7-400 % (for gas standard calibrated VOCs 7-120 %), and the total uncertainty from 33 % to 136 % (for gas standard calibrated VOCs 33-87 %).”

(3)

Section 2.5.7, Fig. S5

Are the authors able to speculate what causes the KL15 footprints being biased way too big/far?

Indeed, I made similar experiences (unpublished). On the other hand, Hannun et al. (2020) appear to have gotten reasonable footprints for their airborne fluxes using KL15. (And they also explicitly write that model is "applicable to many turbulence regimes and measurement heights".) Unfortunately, I have not had time yet to figure out the details in that paper. But I am curious about the applicability of KL15 in general, and about possibly easily occurring oversights or misunderstandings when applying that parametrization. Especially for airborne datasets.

Yes, we have investigated the difference between the KL15 and KL04 models. We even obtained the model input data from Hannun et al. (2020) for comparison. The input parameters of Hannun et al. were in the same range as ours, the main difference being that we were closer to the top of the PBL. Increasing z/zi while keeping all other input parameters from Hannun et al. constant resulted in similarly large footprints (new Table S3).

Additionally, a certain difference is caused by the roughness length. It is possible to run the KL15 model with the roughness length set to "nan", so that it calculates the roughness length from the Obukhov length and the mean horizontal wind speed. This is what Hannun et al. did. We used roughness lengths attributed to our landscape (between 0.075 and 0.5 m) from HRRR. Using such roughness lengths as model input also results in larger footprints (new Table S3). Interestingly, even using a large roughness length, 1 m (typically used for forests), increases the footprint size compared to using "nan", which does not appear reasonable.

We conclude that the KL15 model has a bias towards oversized footprints for measurements obtained close to the top of the PBL, and potentially an issue with the representation of the influence of roughness lengths on the footprint size.

We added the following to the text:

"The KL15 algorithm resulted in overly large footprints for our data (Fig. S5). We investigated this difference to the reasonable footprint sizes obtained with the KL15 model for airborne fluxes by Hannun et al. (2020). The input parameters of our dataset and the Hannun et al. (2020) dataset were in the same ranges (Table S3), except for a) the flight altitude normalized by the boundary layer height (z/z_i), which was significantly higher in our study, and b) the roughness length, which we obtained for the landscape from HRRR (ranging between 0.075 and 0.5 m), while Hannun et al. kept this input parameter empty. (When no roughness length is put in, the algorithm uses the Obukhov length and mean horizontal wind speed to derive the roughness length.) As shown in Table S3, using a higher z/zi while otherwise keeping the Hannun et al. (2020) parameters, also resulted in oversized footprints, even more so when also applying any roughness length. We thus conclude that the KL15 model is biased towards extreme footprint lengths when the measurement height is close to the top of the boundary layer and that footprint lengths are sensitive towards using or not using roughness length input."

And we added the following table to the SI:

Table S3. Comparison of KL15 footprint model input and results between Hannun et al. (2020) and this study. Values are typical ranges. Footprint lengths are given for the 90th percentile footprints. "nan" = not a number.

KL15 input parameters	Hannun et al. (2020)	This study
PBL height (m)	300 – 2000	600 – 1400
Obukhov length (m)	-200 – -500	-100
Standard deviation of lateral velocity σ_v (m/s)	0.6 – 3	0.8 – 1.5
Friction velocity u* (m/s)	0.4 – 1	0.1 – 0.44
Mean horizontal wind speed (m/s)	3 – 10	1 – 6
Aircraft altitude (m)	80 – 300	350 – 550
Roughness length (m)	nan	0.075 – 0.5
KL15 footprint length (km) using means of above values	*15*	*70*

Sensitivity test		
Footprint length (km) after altering the aircraft altitude to 450 m	*47*	
Footprint length (km) after altering the aircraft altitude to 450 m and the PBL height to 1000 m	*57*	
Footprint length (km) after altering the aircraft altitude to 450 m, the PBL height to 1000 m, and the roughness length to 0.5 m	*82*	
Footprint length (km) after altering the aircraft altitude to 450 m, the PBL height to 1000 m, and the roughness length to 1 m	*73*	

(4)

Fig. 3 (and related results; also Section 2.3.3):

Several signals required corrections for fragmentation and/or hydration in the instrument (e.g., 2.3.3). It appears likely then that other signals are subject to similar issues, but which are simply not that well understood. Could such insufficiently understood induced reactions produce biases, in particular in light of the reported overall results (as presented for instance in Fig. 3)? And if so, what kind of biases should be considered? Or are the reported compounds actually well understood in terms of their response to PTR-MS?

This is a valid concern that we took very seriously during our data processing. Firstly, we would like to emphasize that all VOCs that are shown individually in figures and that contribute major discrepancies with the inventories are gas-standard calibrated, and/or well understood, so that interferences can be assumed to be non-existent or minimal. For example, ethanol does not have interferences on its own mass (Coggon et al., 2023) but it fragments onto acetaldehyde which was corrected for. Generally, we were careful to make direct comparisons with the inventory only where we are sufficiently certain that the PTR measurements are not subject to interferences. We consulted the literature (e.g. (Pagonis et al., 2019)) to rule out any substantial interferences. Compounds where such interferences are likely present were not discussed.

Concerning overall results, such as Figure 3: The main contributors to the pie charts are known, calibrated and/or corrected for fragmentation and interferences. We also strived to exclude the

impact even of unknown fragments by searching for strong correlations within the dataset, which is now explained. We added to the text in 2.3.3:

"All VOCs that are shown individually in figures and that contribute most of the flux and/or contribute major discrepancies with the inventories are gas-standard calibrated, and their fragmentation well understood (Pagonis et al., 2019), so that remaining interferences after the above corrections can be assumed to be minimal. We also strived to exclude the impact of unknown fragments by searching for strong correlations within the dataset. Any m/z that correlated with another with an $r^2 > 0.97$ was investigated regarding potential effects of water clustering or fragmentation. If it made chemical sense, the m/z was identified as a fragment or water cluster and consequently added up with its parent m/z. This concerned the following protonated m/z: 61.03 ($C_2H_5O_2$+) with fragment 43.02 (C2H3O+) and water clusters 79.04 (C2H7O3+) and 97.05 (C2H9O4), 87.04 ($C_4H_7O_2$+) with water cluster 105.05 ($C_4H_9O_3$+), 89.02 (C3H5O3+) with water cluster 107.03 ($C_3H_7O_4$+) and fragment 71.01 ($C_3H_3O_2$+), 99.04 ($C_5H_7O_2$+) with water cluster 117.05 ($C_5H_9O_3$+), 101.02 (C_4H_5O3+) with water cluster 119.03 (C4H7O4+), 103.04 (C4H7O3+) with fragment 85.02 (C4H5O2+), 115.07 (C6H11O2+) with water cluster 133.08 (C6H13O3+), 115.11 (C7H15O+) with water cluster 133.12 (C7H17O2+), 125.10 (C8H13O+) with fragment 111.08 (C7H11O+), 129.05 (C6H9O3+) with fragment water cluster 123.03 (C3H7O5+), 141.02 (C6H5O4+) with water cluster 159.03 (C6H7O5+), 143.11 (C8H15O2+) with fragment water cluster 147.01 (C7H15O3+), 159.14 (C9H19O2+) with water cluster 177.15 (C9H21O3+), 229.18 (C13H25O3+) with fragments 173.11 (C9H17O3+) and 191.13 (C9H19O4+). All fragmentation corrections were done in molar units to prevent biases in the mass flux.

However, we cannot completely confirm having found all fragments. Consequently, the "other C_xH_y" or the "alkenes" groups (Fig. 3) may partly consist of fragments of OVOCs while some m/z identified as OVOCs may be water clusters. The overall composition discussed in Sect. 3.1 is not expected to be impacted by such minor impacts."

Minor comments:

L65-67: Were all "4-6 different altitudes" within the PBL flown inside the 300-400 m AGL range, or does that range only refer to the lowest racetracks? (In the latter case, how high did the stacks reach?)

The top of the PBL was first determined by a sounding, i.e. by a flight leg with a steep increase in altitude. By watching the dewpoint temperature and water concentration, we thus roughly determined the PBL height in flight and stopped the ascent when we had found the top of the PBL. From this PBL height, we calculated evenly-spaced altitudes within the PBL to fly the racetrack patterns at. We hope the following text addition makes this clearer:

"Every other flight included a 12-15 km long stacked racetrack pattern (Karl et al., 2013) flown at 4-6 altitudes evenly spaced between ≈300 m and the top of the planetary boundary layer (PBL), the local height of which was determined by a sounding preceding the racetrack pattern."

L105+: Maybe the authors could briefly put the instrument parameters (in particular the E/N) into perspective for the reader less familiar with the instrumentation. E.g., what kind of

instrument behavior is desired/expected/achieved from an E/N of 130 Td, or a potential gradient of 590 V?

We altered the text to explain this better:

"The Vocus proton transfer reaction time of flight mass spectrometer (Vocus PTR-ToF-MS, Aerodyne Inc., Billerica, MA, USA, (Krechmer et al., 2018)) was operated at 2.0 mbar reactor pressure, 60°C reactor temperature, a potential gradient along the focusing ion-molecule reactor (FIMR) of 590 V and a resulting E/N of ca. 130 Td. This E/N is expected to cause only moderate fragmentation (Yuan et al., 2017). Unlike with traditional PTR-MS instruments, in the Vocus instrument the fragmentation rate is strongly (often more strongly than by E/N) affected by the gradient between skimmer 1 and skimmer 2 (or between skimmer 1 and BSQ front voltage) (Coggon et al., 2023). The difference between skimmer 1 and skimmer 2 was changed once during the campaign from 6 to 9.1 V, which resulted in an improved sensitivity for some VOCs (e.g., methanol, which is prone to water clustering), but stronger fragmentation for others (e.g., monoterpenes, sesquiterpenes and nonanal), both of which effects were accounted for through calibration. The mass resolution was ≈4800 ± 280 (average ± standard deviation). The reagent water flow was 20 sccm, resulting in a high water mixing ratio (10 %v/v–20 %v/v) in the FIMR, so that the instrument showed no humidity dependence in its sensitivity. This is an advantage in flux measurements because it eliminates the necessity to correct for humidity differences between different eddies caused by water fluxes. The high water mixing ratio causes a large primary ion (H_3O^+) signal, which is lowered by a big segmented quadrupole (BSQ) that reduces the transmission of low-mass ions in order not to wear down the detector too quickly. However, we kept the voltage of the BSQ relatively low at 200 V so that low-mass VOCs like methanol could be detected with reasonable sensitivity. The methanol sensitivity was on average 58 cps/ppb for the low skimmer voltage difference setting and 136 cps/ppb for the high skimmer voltage difference setting."

L131: Regarding the sensitivity estimation "for all m/z without a corresponding gas standard", could the authors provide a reference for more details on that procedure?

We added a reference and more details:

"For all m/z without a corresponding gas standard, the sensitivities were derived from a theoretical calibration, using a root function (the expected function of a ToF transmission) fitted to reaction rate normalized sensitivities of non-fragmenting and non-clustering gas-standard calibrated VOCs (Jensen et al., 2023; Holzinger et al., 2019). This approach accounts for transmission effects dependent on m/z. The uncertainties of this and the gas-standard calibration are based on typical estimates for the uncertainty of the theoretical calibration (50%) and the gas-standard calibration uncertainty (20%), which consists of the calibration standard uncertainty and the uncertainty of the mass flow controller. The resulting estimated uncertainty of the calibration for gas-standard calibrated VOCs was 20%, while it was 54% for all other VOCs (propagated from 20% and 50%)."

2.3.3
I suggest to consider also the recent findings by Vermeuel et al. (https://doi.org/10.5194/acp-23-4123-2023) regarding corrections they needed for deriving isoprene based on the C5H9+ signal. I am quite convinced of the correction method applied here, but worth double-checking.

Our isoprene correction agrees with the findings of Vermeul et al., who also corrected for n-aldehydes that fragment on the isoprene mass. Different from our study, they had GC data to base their correction on. We applied our corrections following Coggon et al. (2023), a study that compared a GC-based correction with a correction based on the m/z 111 and m/z 125 fragments and found that they agree. Therefore, we are confident that our correction based on m/z 111 and m/z 125 is robust.

We added references to Vermeul and Coggon to the text:

"Furthermore, longer-chain aldehydes, such as nonanal, also fragment onto C5H8H+ (Buhr et al., 2002; Vermeuel et al., 2023). Such aldehydes may be relevant in dairy emissions (Rabaud et al., 2003). Fragments of both the long-chain aldehydes and the cycloalkanes also appear on C8H15+ (m/z 111.12) and/or C9H17+ (m/z 125.13) which can therefore be used for correction (Coggon et al., 2023). To distinguish isoprene from interfering fragments of aldehydes and cycloalkanes, we used an approach following the findings of Coggon et al."

L172: Unclear to me how that re-speciation was done, and if it was a result of this study or based on something else. Could the authors provide a little more detail, or a reference either to another study or to the section where that is discussed in more detail here?

The re-speciation is independent of this study and is described in Table R1 (also Table S6 in Zhu et al., 2023, in prep). We added a reference to the text: "We also re-speciated the FIVE-VCP inventory to the updated RACM2_Berkeley2.0 mechanism (Zhu et al., in prep)."

Emission Category	Full Name	RACM_ESRL_VCP		RACM2B-VCP	
		Name	Weight	Name	Weight
CO	CO	e_co	1.00	e_co	1.00
	NO	e_no	0.90	e_no	0.90
NOX	NO2	e_no2	0.092	e_no2	0.092
	HONO	e_hono	0.008	e_hono	0.008
SO2	SO2	e_so2	1.00	e_so2	1.00
NH3	NH3	e_nh3	1.00	e_nh3	1.00
HC01	Methane	e_ch4	1.00	e_ch4	1.00
HC02	Ethane, kOH<500 /ppm/min	e_eth	1.00	e_eth	1.00
HC03	Alkane 500<kOH<2500 exclude(C3H8,C2H2,ethanol,acids)	e_hc3	1.00	e_hc3	1.00
HC04	Alkane 2500<kOH<5000 exlude(butanes)	e_hc3	1.11	e_hc3	1.11
HC05	Alkane 5000<kOH<10000 exlude(pentanes)	e_hc5	0.97	e_hc5	0.97
HC06	Alkane kOH>10000 exclude(ethylene glycol)	e_hc8	1.00	e_hc8	1.00
HC07	Ethylene	e_ol2	1.00	e_ol2	1.00
HC08	Alkene kOH <20000 /ppm/min	e_olt	1.00	e_olt	1.00
HC09	Alkene kOH >20000 /ppm/min exclude(dienes,styrenes)	e_oli	1.00	e_oli	1.00
HC10	Isoprene	e_iso	1.00	e_iso	1.00
HC11	Anthro terpenes (VCPs 7/3/19)	e_terp	1.00	e_terp	1.00
HC12	Aromatic kOH <20000 /ppm/min exclude(benzene and toluene)	e_tol	1.00	e_ben e_tol	0.80 0.80
HC13	Aromatic kOH >20000 /ppm/min exclude(xylenes)	e_xyl	1.00	e_xyl e_xyo	0.67 0.33
HC14	Formaldehyde	e_hcho	1.00	e_hcho	1.00
HC15	Acetaldehyde	e_ald	1.00	e_acd	1.00
HC16	Higher aldehydes	e_ald	1.00	e_ald	1.00
HC17	Benzaldehyde	e_ald	1.00	e_bald	1.00
HC18	Acetone	e_act	1.00	e_act	1.00
HC19	Methylethyl ketone	e_ket	1.61	e_mek	1.00
HC20	PRD2 SAPRAC species (aromatic ketones)	e_ket	1.61	e_ket	1.61
HC21	Methanol	e_moh	1.00	e_moh	1.00
HC22	Glyoxal	e_gly	1.00	e_gly	1.00
HC23	Methylglyoxal	e_mgly	1.00	e_mgly	1.00
HC24	Biacetyl	e_mgly	1.00	e_mgly	1.00
HC25	Phenols	e_csl	1.00	e_phen	1.00
HC26	Cresols	e_csl	1.00	e_csl	1.00
HC27	Methacrolein	e_macr	1.00	e_macr	1.00
HC28	Methylvinyl ketone	e_macr	1.00	e_mvk	1.00
HC29	IPRD SAPRAC species (>C4 unsaturated aldehydes)	e_ket	1.00	e_ket	1.00
HC30	Formic Acid add 1/10/2023	e_ora1	1.00	e_ora1	1.00
HC31	Acetic Acid	e_ora2	1.00	e_ora2	1.00
HC32	>C2 Acids (SAPRC PACD species)	e_ora2	1.00	e_ora2	1.00
HC33	Xylenols (SAPRC-11 species)	e_csl	1.00	e_csl	1.00
HC34	Catechols (SAPRC-11 species)	e_csl	1.00	e_mct	1.00
HC36	Propylene	e_olt	1.00	e_olt	1.00
HC37	Acetylene	e_hc3	0.40	e_ace	1.00
HC38	Benzene	e_tol	0.29	e_ben	1.00
HC39	Butanes	e_hc3	1.11	e_hc3	1.11
HC40	Pentanes	e_hc5	0.97	e_hc5	0.97
HC41	Toluene	e_tol	1.00	e_tol	1.00
HC42	m-Xylene	e_xyl	1.00	e_xyl	1.00
HC43	o-Xylene	e_xyl	1.00	e_xyo	1.00
HC44	p-Xylene	e_xyl	1.00	e_xyl	1.00
HC45	Propane	e_hc3	0.87	e_hc3	0.87
HC46	Dienes	e_oli	1.00	e_dien	1.00
HC47	Styrenes	e_olt	1.00	e_olt	1.00
HC48	Ethanol	e_eoh	1.00	e_eoh	1.00
HC49	Ethylene Glycol	e_eteg	1.00	e_eteg	1.00
PM01	Unspeciated primary PM2.5 - nuclei mode Unspeciated primary PM2.5 - accumulation mode	e_pm25i e_pm25j	0.20 0.80	e_pm25i e_pm25j	0.20 0.80
PM02	Sulfate PM2.5 - nuclei mode Sulfate PM2.5 - accumulation mode	e_so4i e_so4j	0.20 0.80	e_so4i e_so4j	0.20 0.80
PM03	Nitrate PM2.5 - nuclei mode Nitrate PM2.5 - accumulation mode	e_no3i e_no3j	0.20 0.80	e_no3i e_no3j	0.20 0.80
PM04	Organic Carbon PM2.5 - nuclei mode Organic Carbon PM2.5 - accumulation mode	e_orgi e_orgj	0.20 0.80	e_orgi e_orgj	0.20 0.80
PM05	Elemental Carbon PM2.5 - nuclei mode Elemental Carbon PM2.5 - accumulation mode	e_eci e_ecj	0.20 0.80	e_eci e_ecj	0.20 0.80
PM06	Non-Carbon Organic, PM2.5 - nuclei mode Non-Carbon Organic, PM2.5 - accumulation mode	e_orgi e_orgj	0.20 0.80	e_orgi e_orgj	0.20 0.80
PM10-PRI	Unspeciated Primary PM10	e_pm10	1.00	e_pm10	1.00
CO2	CO2	e_co2	1.00	e_co2	1.00
HC50	Unidentified/Unknown VOC - to go into IVOC for SOA 10/2/18	e_unid	1.00	e_unid	1.00
HC51	Isopropyl Alcohol, Oxygenated VCP add 8/2/20	e_ipoh	1.00	e_ipoh	1.00
HC52	Propylene Glycol, Oxygenated VCP add 8/2/20	e_prog	1.00	e_prog	1.00
HC53	Glycerol, Oxygenated VCP add 8/2/20	e_glyc	1.00	e_glyc	1.00
HC54	D4-Siloxane add 8/10/22	e_tol	0.29	e_d4silx	1.00
HC55	D5-Siloxane add 8/10/22	e_tol	0.29	e_d5silx	1.00
HC56	Other Siloxane add 8/10/22	e_tol	0.29	e_ben	1.00
HC57	NROG add 8/10/22	e_nrog	1.00	e_nrog	1.00
HC58	pchtf add 8/10/22	e_nrog	1.00	e_pchtf	1.00
HC59	pdchx add 8/10/22	e_nrog	1.00	e_pdchx	1.00
HC60	Propanal add 8/10/22	e_ald	1.00	e_cald	1.00
HC61	Butanal add 8/10/22	e_ald	1.00	e_cald	1.00
HC62	Pentanal add 8/10/22	e_ald	1.00	e_cald	1.00
HC63	Hexanal add 8/10/22	e_ald	1.00	e_cald	1.00
HC64	Heptanal add 8/10/22	e_ald	1.00	e_cald	1.00
HC65	Octanal (and C10+ aldehydes) add 8/10/22	e_ald	1.00	e_cald	1.00
HC66	Nonanal add 8/10/22	e_ald	1.00	e_cald	1.00
HC67	Unsaturated Aldehydes add 8/10/22	e_macr	1.00	e_cuald	1.00
HC68	C10+ aldehydes add 11/4/22	e_ald	1.00	e_cald	1.00

Table R1: The species mapping between FIVE-VCP emission inventory and two chemical mechanisms used in WRF-Chem, RACM-ESRL-VCP and RACM2B-VCP (updated RACM2_Berkeley2.0 mechanism in the context).

L200: I assume so, but was the scale bias correction applied (e.g., Liu et al., 2007)?

Yes, it is part of the procedure. We added this information and the reference to the text.

L235-236: There is reference to references in Table S1. Where are these references? I fail to find them.

We apologize for this oversight. The new Table S1 includes the references.

L238+: It would be very interesting to see an example or summary of that verification. Also, which monoterpene oxidation products and ratios were used and expected? (Probably best in the supplement.)

We added a description and figure to the supplement and made additions to the main text:

"The speciation of monoterpenes measured as C10H16H+ was assumed to be the same as the monoterpene composition in Pusede et al. (2014) (Table S1). The resulting reaction rate was verified by comparing (i) the median ratio of inferred surface flux (after O3 and OH correction) to measured aircraft flux at altitude (1.2), with the ratio of extrapolated surface flux vs. flux at flight altitude in stacked racetrack fluxes (1.2-1.4), and (ii) the monoterpene oxidation product/monoterpene ratio with expected yields according to the reaction rate used (Text S1, Fig. S7)."

"Text S1: Description of the back-of-the-envelope calculation for verification of the monoterpene composition

Apart from extrapolating vertical monoterpene flux gradients to the ground (see main text), we used a second method to verify that the assumed monoterpene composition agrees with the observed monoterpene oxidation rates. This method relies on the ratio of observed monoterpene mixing ratios towards a monoterpene oxidation product. The only monoterpene oxidation product that we deemed eligible for such a comparison was $C_9H_{14}O$ (m/z 139.11) which consists of major monoterpene oxidation products such as limona ketone, limonene aldehyde, nopinone, and sabina ketone. Other monoterpene oxidation product masses, e.g., m/z 153.13 ($C_{10}H_{16}O$), also include directly emitted monoterpenoids such as citral or camphor and are therefore not suitable for oxidation product-to-precursor ratios.

With a median OH concentration of 2.8e6 molec/cm³, approximate yields of 50% for the formation of the $C_9H_{14}O$ products from limonene, sabinene and b-pinene (Calogirou et al., 1999), as well as a median ozone concentration of 1.11e12 molec/cm³ with a yield of 17% from the ozone reaction (Calogirou et al., 1999), and a transport time of 336 s (convective velocity scale 1.2 m/s x 427 m observation altitude), we can expect the formation of approximately 0.03 ppb $C_9H_{14}O$ from each ppb of $C_{10}H_{16}$ monoterpene based on the reaction rates of k_{OH} = 5.91e-11 cm³/(molec s) and k_{O3} = 9.59e.17 cm³/(molec s). This is in reasonable agreement with the ratio of $C_9H_{14}O$ vs. $C_{10}H_{17}$ observed (slope = 0.047, Fig. S7)."

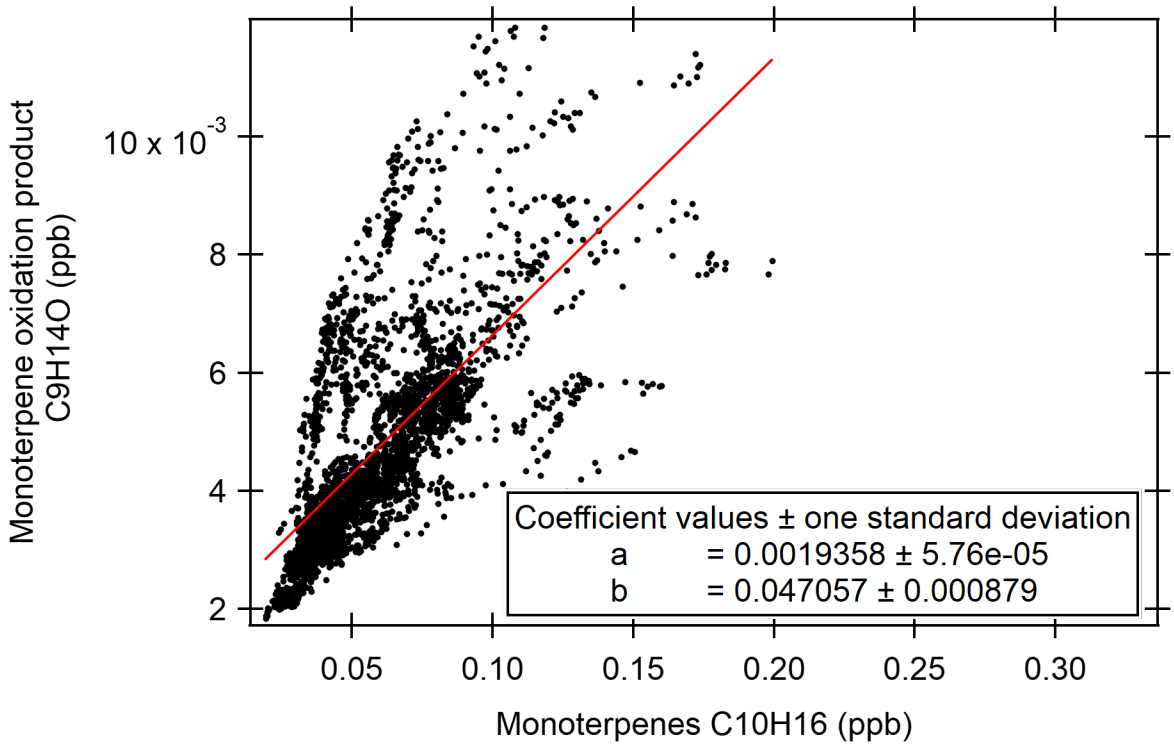

Figure S7: Monoterpenes (C10H16) mixing ratio vs. monoterpene oxidation product (C9H14O) mixing ratio for flight SJV7. The coefficients for the equation y = a+bx are shown in the box.

L260: Should probably specify that the "intercept" means the x-intercept.

We clarified the whole derivation of the equation as follows:

"The vertical divergence slope (s) is determined from a linear regression of the median flux of each altitude bin vs. z/z_i (Fig. S2 shows x and y axis inverted).

The linear equation for a flux at altitude z (F_z) can be expressed as:

$$F_z = F_0 + s\frac{z}{z_i} \quad (4)$$

The slope is normalized by the intercept with the flux axis F_0 (which corresponds to the surface flux), and we call the normalized slope: $s/F_0 = C$.

$$\frac{F_z}{F_0} = 1 + C\frac{z}{z_i} \quad (5)$$

Rearranging the equation, the surface fluxes (F_0) can be calculated from the fluxes at altitude z as:

$$F_0 = \frac{F_z}{1+C\cdot\frac{z}{z_i}} \quad (6)"$$

2.5.4 + Fig. S2 + Table S1:

I probably get something wrong here, indicating that the section could be clarified somewhere. E.g., for benzene, slope is -0.0741 and intercept is 0.0838, so C is -0.884 and the correction factor should be (Eq. 4) between 1.21 (z/zi=0.2) and 2.4 (z/zi=0.66). But Table S1 lists a factor of 0.013 (though with an uncertainty of 1.24). Was the physical flux divergence simply quite variable between flights? (Or uncertain?) And Fig. S2 only showing the data for one flight?) ... Oh, Section 2.5.6 actually indicates only moderate variability... I remain confused.

We apologize for this confusion caused by an error in the table export and are very grateful that you have found it. Due to an error in the table export code, some table headers were shifted to the wrong columns. The new version of Table S1 shows a mean divergence correction for benzene of 1.4, which agrees with the reviewer's correct calculation. We also hope that the additions described in our response to your comment on L260 help clarify this paragraph further.

Fig. 1: The footprints are presumably a campaign-long average? Not clear.

No, they are not. We changed the caption: "Footprints along the flight tracks for each observed flux measurement during the campaign (therefore, overlaps exist). …"

Technical comments:

Fig. 1:

I am worried that the (important) geographic labels will become unreadable in the final version.

Thanks for pointing this out. We updated the figure with larger labels.

Fig. S2:

What do the dashed lines show?

They show 95% confidence intervals. We now made this clear in the caption.

Reviewer 3

This manuscript shows the results of airborne eddy covariance flux in California. The authors demonstrates that the airborne eddy covariance technique can provide valuable information for improve emission inventory. I recommend the manuscript is published in ACP after some minor modifications.

We thank the reviewer for the positive assessment and the helpful comments which helped improve this manuscript. Responses below in blue, changes to the manuscript in red.

1. Line 84: Naval Postgraduate School (NPS)

Changed.

2. Line 108 and Line 113-114: The status of PTR instrument is well controlled by factors about pressures and voltages of several key modules, which has been well acknowledged by the community. Without further explanation of reasons and theories, it might be better to provide more information of the specific compounds that were involved in the evaluation of status change as guidance for the readers and colleagues in the community.

   Which VOCs received improved sensitivity and which VOCs experienced high branching during the adjustment of the gradient between skimmer 1 and skimmer 2 from 6 to 9.1 V?

   As the amount of primary ion was limited by reducing the transmission of low-mass ions, specific number will be more helpful. What is the sensitivity of methanol with BSQ = 200 V that can be recognized as reasonable?

We altered the text to explain this better:

"The Vocus proton transfer reaction time of flight mass spectrometer (Vocus PTR-ToF-MS, Aerodyne Inc., Billerica, MA, USA, (Krechmer et al., 2018)) was operated at 2.0 mbar reactor pressure, 60°C reactor temperature, a potential gradient along the focusing ion-molecule reactor (FIMR) of 590 V and a resulting E/N of ca. 130 Td. This E/N is expected to cause only moderate fragmentation (Yuan et al., 2017). Unlike with traditional PTR-MS instruments, in the Vocus instrument the fragmentation rate is strongly (often more strongly than by E/N) affected by the gradient between skimmer 1 and skimmer 2 (or between skimmer 1 and BSQ front voltage) (Coggon et al., 2023). The difference between skimmer 1 and skimmer 2 was changed once during the campaign from 6 to 9.1 V, which resulted in an improved sensitivity for some VOCs (e.g., methanol, which is prone to water clustering), but stronger fragmentation for others (e.g., monoterpenes, sesquiterpenes and nonanal), both of which effects were accounted for through calibration. The mass resolution was ≈4800 ± 280 (average ± standard deviation). The reagent water flow was 20 sccm, resulting in a high water mixing ratio (10 %v/v–20 %v/v) in the FIMR, so that the instrument showed no humidity dependence in its sensitivity. This is an advantage in

flux measurements because it eliminates the necessity to correct for humidity differences between different eddies caused by water fluxes. The high water mixing ratio causes a large primary ion (H_3O^+) signal, which is lowered by a big segmented quadrupole (BSQ) that reduces the transmission of low-mass ions in order not to wear down the detector too quickly. However, we kept the voltage of the BSQ relatively low at 200 V so that low-mass VOCs like methanol could be detected with reasonable sensitivity. The methanol sensitivity was on average 58 cps/ppb for the low skimmer voltage difference setting and 136 cps/ppb for the high skimmer voltage difference setting."

3. Line 131-133: Citations are needed for this root function method for the sensitivity determination of VCOs without gas-standard.

We added a reference and more details:

"For all m/z without a corresponding gas standard, the sensitivities were derived from a theoretical calibration, using a root function (the expected function of a ToF transmission) fitted to reaction rate normalized sensitivities of non-fragmenting and non-clustering gas-standard calibrated VOCs (Jensen et al., 2023; Holzinger et al., 2019). This approach accounts for transmission effects dependent on m/z. The uncertainties of this and the gas-standard calibration are based on typical estimates for the uncertainty of the theoretical calibration (50%) and the gas-standard calibration uncertainty (20%), which consists of the calibration standard uncertainty and the uncertainty of the mass flow controller. The resulting estimated uncertainty of the calibration for gas-standard calibrated VOCs was 20%, while it was 54% for all other VOCs (propagated from 20% and 50%)."

4. Section 2.3.3: The signal interference of PTR instruments due to fragmentation and clustering can be quite complicated. Interference correction was done in a reasonable method as mentioned by authors but could you quantify the interference for isoprene and acetaldehyde? Such how much difference the interference correction brought in terms of isoprene mixing ratios? And acetaldehyde?

More details on these corrections and their size for our campaign can also be found in Coggon et al. (2023). We added the requested information:

"For an accurate isoprene flux correction, this equation was applied to the fluxes of m/z 69.07 and (m/z 111.12 + m/z 125.13) directly, not to the mixing ratios first, resulting in a median of 12% reduction of the isoprene flux, and a 48% reduction in the isoprene mixing ratio. Similarly, acetaldehyde was corrected for ethanol fragments (Coggon et al., 2023), resulting in a 26% reduction (both flux and mixing ratio)."

5. Line 184-185: Citation of this PBL estimation method is needed.

We added a reference to Karl et al. (2013).

6. Line 194-198: I understand that due to the low actual flux of some VOCs, it was hard to derive the lag time by checking the covariance peak above the noise. Applying the lag time of isoprene for VOCs with low signal to noise ratio can be one answer but, in such way, the variation of stickiness would be neglected. Therefore, it would be better to provide the variation of lag time for multiple VOCs, including cresol, ethanol and nonanal, to show how much difference there would be in term of the impact of stickiness variation.

We agree that this method is not perfect, however we decided it was the most reasonable approach to use in the case of this field campaign. The assumption is that when the signal to noise ratio is so low that no covariance peak can be found within the +/- 4 s window (which should be plenty even for sticky VOCs), there is usually no actual flux. Unfortunately, the lag times of the sticky VOCs were so variable that assigning *any* lag time would likely not have improved the result.

We added to the text in Sect. 2.5.2:

"For instance, mean lag times (± standard deviation) where the flux was above the 3σ detection limit were for isoprene 0.004 ± 1.07 s, for toluene 0.13 ± 0.46 s, for ethanol 0.32 ± 1.04 s, for nonanal 0.69 ± 2.54 s, and for cresol 1.66 ± 1.92 s. "

7. Line 237: The speciation analysis of monoterpenes is one of the examples. The determination of OH reaction coefficient for other isobaric compounds should be involved in the discussion, especially the impact of OH reaction coefficient selection on the flux divergence correction.

We agree this is an important point to mention and you made us realize that we had not mentioned how we derived OH reaction rate coefficients for each of the m/z measured, so we added more explanation to Sect. 2.5.3. However, the physical vertical divergence correction is likely a much larger source of error than the chemical vertical divergence correction since 1) the transport time between surface and point of observation was short enough that only few VOCs required significant correction for oxidative loss (Table S1 shows the median oxidation correction as a fraction of the flux), and 2) most isomeric compounds except the terpenes have relatively similar OH reaction rates (within 10-50%). This is especially true for the OVOCs (Isaacman-VanWertz and Aumont, 2021), which are the largest group of unidentified isomeric compounds here. On the other hand, the uncertainty of the vertical divergence correction is on the order of 100%.

The following additions to 2.5.3 were made:

"For m/z that could be attributed to several isomers, we generally used the average reaction rate coefficient of all potential isomers following Pfannerstill et al. (2021 and 2019), and if there was

no reaction rate coefficient available, we used the recommended values from Isaacman-VanWertz and Aumont (2021) for VOCs containing O, N, or O and N atoms."

And

"Generally, the magnitude of the chemical vertical divergence correction depends on the oxidation rate applied in Eq. 2. PTR-ToF-MS cannot separate isomers, so the oxidation rates attributed to each m/z are based on best estimates. However, for most VOCs the chemical vertical divergence correction was negligibly small (Table S1) since most of them (no matter which isomer) are longer lived than the transport time between the surface and the point of observation. Therefore, the only VOCs where the uncertainty of the chemical composition caused significant uncertainty in the final flux were the sesquiterpenes and monoterpenes. For a discussion of uncertainties, see Sect. 2.5.6."

8. Line 310: What is the grid size of CARB inventory and FIVE-VCP inventory? What was the strategy to downscale the inventory data to higher spatial resolution if required?

It is already mentioned in Sect. 2.6 that both inventories are at 4 km grid size, but we clarified this again in another place:

"For VOC flux comparison with the inventory, each footprint (corresponding to a measured flux) was matched to the 4 km x 4 km inventory grid cells that it overlapped with…"

We did not downscale the inventory data. Instead, we matched the footprints to the 4x4 km cell size, not vice versa. We hope an addition to the text makes this clearer:

"For VOC flux comparison with the inventory, each footprint (corresponding to a measured flux) was matched to the 4 km x 4 km inventory grid cells that it overlapped with, weighted by the percentage of the overlap, if the overlap was > 10 % of the area of the grid cell and the sum of all overlaps amounted to at least 100 %. The measured and inventory data for each grid cell were matched in time. Thus, we obtained time-resolved 4 km x 4 km gridded fluxes from the measurements. Only for the purpose of plotting maps, an average of all flyovers was calculated for each grid cell."

9. Line 320: Based on the description in Line 237, the speciation of monoterpenes followed the same composition in Pusede et al., 2014 and Lu et al., 2019. It might be better to show the specific composition somewhere in the SI, since the OH reaction rate coefficient of d-limonene is three times of the one of a-pinene, which would make great difference in later valuation, such as Line 368 and Line 496.

We added the explicit monoterpene composition to Table S1:

Monoterpenes (30% a-pinene, 14% d3-carene, 36% sabinene, 4% camphene, 2% b-pinene, 14% limonene).

10. Section 3.4: It would be necessary to add words about how the inventory deals with the temperature dependence of the emission of certain compounds before showing Figure 11.

Thank you for this suggestion. We added to the text in Sect. 3.4:

"The inventories parameterize biogenic emissions based on dependence to temperature and light (Guenther et al., 2012). Anthropogenic emissions are not explicitly parameterized for dependence on temperature. Instead, their temperature dependence is accounted for through the application of average seasonal and diurnal temporal profiles across various VOC emission sources."

Additional revision of our own accord: We would like to add the word "agricultural" to the title so that people looking for studies of agricultural VOCs have an easier time finding it. So, the new title would be: "Volatile organic compound fluxes in the agricultural San Joaquin Valley – spatial distribution, source attribution, and inventory comparison"

References

Calogirou, A., Larsen, B. R., and Kotzias, D.: Gas-phase terpene oxidation products: a review, ATMOSPHERIC ENVIRONMENT, 33, 1423–1439, https://doi.org/10.1016/S1352-2310(98)00277-5, 1999.

Coggon, M. M., Stockwell, C. E., Claflin, M. S., Pfannerstill, E. Y., Xu, L., Gilman, J. B., Marcantonio, J., Cao, C., Bates, K. H., Gkatzelis, G. I., Lamplugh, A., Katz, E. F., Arata, C., Apel, E. C., Hornbrook, R. S., Piel, F., Majluf, F., Blake, D. R., Wisthaler, A., Canagaratna, M. R., Lerner, B. M., Goldstein, A. H., Mak, J. E., and Warneke, C.: Identifying and correcting interferences to PTR-ToF-MS measurements of isoprene and other urban volatile organic compounds, submitted to Atmos. Meas. Tech., 2023.

Guenther, A. B., Jiang, X., Heald, C. L., Sakulyanontvittaya, T., Duhl, T., Emmons, L. K., and Wang, X.: The Model of Emissions of Gases and Aerosols from Nature version 2.1 (MEGAN2.1): An extended and updated framework for modeling biogenic emissions, Geosci. Model Dev., 5, 1471–1492, https://doi.org/10.5194/gmd-5-1471-2012, 2012.

Hannun, R. A., Wolfe, G. M., Kawa, S. R., Hanisco, T. F., Newman, P. A., Alfieri, J. G., Barrick, J., Clark, K. L., DiGangi, J. P., Diskin, G. S., King, J., Kustas, W. P., Mitra, B., Noormets, A., Nowak, J. B., Thornhill, K. L., and Vargas, R.: Spatial heterogeneity in CO 2 CH 4 and energy fluxes: insights from airborne eddy covariance measurements over the Mid-Atlantic region, Environ. Res. Lett., 15, 35008, https://doi.org/10.1088/1748-9326/ab7391, 2020.

Holzinger, R., Acton, W. J. F., Bloss, W. J., Breitenlechner, M., Crilley, L. R., Dusanter, S., Gonin, M., Gros, V., Keutsch, F. N., Kiendler-Scharr, A., Kramer, L. J., Krechmer, J. E., Languille, B., Locoge, N., Lopez-Hilfiker, F., Materić, D., Moreno, S., Nemitz, E., Quéléver, L. L. J., Sarda Esteve, R., Sauvage, S., Schallhart, S., Sommariva, R., Tillmann, R., Wedel, S., Worton, D. R., Xu, K., and Zaytsev, A.: Validity and limitations of simple reaction kinetics to calculate concentrations of organic compounds from ion counts in PTR-MS, Atmos. Meas. Tech., 12, 6193–6208, https://doi.org/10.5194/amt-12-6193-2019, 2019.

Isaacman-VanWertz, G. and Aumont, B.: Impact of organic molecular structure on the estimation of atmospherically relevant physicochemical parameters, Atmos. Chem. Phys., 21, 6541–6563, https://doi.org/10.5194/acp-21-6541-2021, 2021.

Jensen, A. R., Koss, A. R., Hales, R. B., and Gouw, J. A. de: Measurements of VOCs in ambient air by Vocus PTR-TOF-MS: calibrations, instrument background corrections, and introducing a PTR Data Toolkit, Atmos. Chem. Phys. Discuss., https://doi.org/10.5194/egusphere-2023-842, 2023.

Krechmer, J., Lopez-Hilfiker, F., Koss, A., Hutterli, M., Stoermer, C., Deming, B., Kimmel, J., Warneke, C., Holzinger, R., Jayne, J., Worsnop, D., Fuhrer, K., Gonin, M., and Gouw, J. de: Evaluation of a New Reagent-Ion Source and Focusing Ion-Molecule Reactor for Use in Proton-Transfer-Reaction Mass Spectrometry, Analytical chemistry, 90, 12011–12018, https://doi.org/10.1021/acs.analchem.8b02641, 2018.

Langford, B., Acton, W., Ammann, C., Valach, A., and Nemitz, E.: Eddy-covariance data with low signal-to-noise ratio: time-lag determination, uncertainties and limit of detection, Atmos. Meas. Tech., 8, 4197–4213, https://doi.org/10.5194/AMT-8-4197-2015, 2015.

Lenschow, D. H., Mann, J., and Kristensen, L.: How Long Is Long Enough When Measuring Fluxes and Other Turbulence Statistics?, J. Atmos. Oceanic Technol., 11, 661–673, https://doi.org/10.1175/1520-0426(1994)011<0661:HLILEW>2.0.CO;2, 1994.

Pagonis, D., Sekimoto, K., and Gouw, J. de: A Library of Proton-Transfer Reactions of H3O+ Ions Used for Trace Gas Detection, Journal of The American Society for Mass Spectrometry, 30, 1330–1335, https://doi.org/10.1007/s13361-019-02209-3, available at: https://doi.org/10.1007/s13361-019-02209-3, 2019.

Pfannerstill, E. Y., Reijrink, N. G., Edtbauer, A., Ringsdorf, A., Zannoni, N., Araújo, A., Ditas, F., Holanda, B. A., Sá, M. O., Tsokankunku, A., Walter, D., Wolff, S., Lavrič, J. V., Pöhlker, C., Sörgel, M., and Williams, J.: Total OH reactivity over the Amazon rainforest: variability with temperature, wind, rain, altitude, time of day, season, and an overall budget closure, Atmos. Chem. Phys., 21, 6231–6256, https://doi.org/10.5194/acp-21-6231-2021, 2021.

Pfannerstill, E. Y., Wang, N., Edtbauer, A., Bourtsoukidis, E., Crowley, J. N., Dienhart, D., Eger, P. G., Ernle, L., Fischer, H., Hottmann, B., Paris, J.-D., Stönner, C., Tadic, I., Walter, D., Lelieveld, J., and Williams, J.: Shipborne measurements of total OH reactivity around the Arabian Peninsula and its role in ozone chemistry, Atmospheric Chemistry and Physics, 19, 11501–11523, https://doi.org/10.5194/acp-19-11501-2019, available at: https://www.atmos-chem-phys.net/19/11501/2019/acp-19-11501-2019.pdf, 2019.

Schobesberger, S., D'Ambro, E. L., Vettikkat, L., Lee, B. H., Peng, Q., Bell, D. M., Shilling, J. E., Shrivastava, M., Pekour, M., Fast, J., and Thornton, J. A.: Airborne flux measurements of ammonia over the southern Great Plains using chemical ionization mass spectrometry,

Atmos. Meas. Tech., 16, 247–271, https://doi.org/10.5194/amt-16-247-2023, available at: https://amt.copernicus.org/articles/16/247/2023/, 2023.

Wolfe, G. M., Hanisco, T. F., Arkinson, H. L., Bui, T. P., Crounse, J. D., Dean-Day, J., Goldstein, A., Guenther, A., Hall, S. R., Huey, G., Jacob, D. J., Karl, T., Kim, P. S., Liu, X., Marvin, M. R., Mikoviny, T., Misztal, P. K., Nguyen, T. B., Peischl, J., Pollack, I., Ryerson, T., St. Clair, J. M., Teng, A., Travis, K. R., Ullmann, K., Wennberg, P. O., and Wisthaler, A.: Quantifying sources and sinks of reactive gases in the lower atmosphere using airborne flux observations, Geophys. Res. Lett., 42, 8231–8240, https://doi.org/10.1002/2015GL065839, 2015.

Wolfe, G. M., Kawa, S. R., Hanisco, T. F., Hannun, R. A., Newman, P. A., Swanson, A., Bailey, S., Barrick, J., Thornhill, K. L., Diskin, G., DiGangi, J., Nowak, J. B., Sorenson, C., Bland, G., Yungel, J. K., and Swenson, C. A.: The NASA Carbon Airborne Flux Experiment (CARAFE): instrumentation and methodology, Atmos. Meas. Tech., 11, 1757–1776, https://doi.org/10.5194/AMT-11-1757-2018, 2018.

Yuan, B., Koss, A. R., Warneke, C., Coggon, M., Sekimoto, K., and Gouw, J. A. de: Proton-Transfer-Reaction Mass Spectrometry: Applications in Atmospheric Sciences, Chemical reviews, 117, 13187–13229, https://doi.org/10.1021/acs.chemrev.7b00325, 2017.

Zhu, Q., Place, B., Pfannerstill, E. Y., Tong, S., Zhang, H., Wang, J., Nussbaumer, C. M., Wooldridge, P., Schulze, B. C., Arata, C., Bucholtz, A., Seinfeld, J. H., Goldstein, A. H., and Cohen, R. C.: Direct observations of NO x emissions over the San Joaquin Valley using airborne flux measurements during RECAP-CA 2021 field campaign, Atmos. Chem. Phys. Discuss., 1–21, https://doi.org/10.5194/acp-2023-3, 2023.